Chemical Geology 582 (2021) 120410

Contents lists available at ScienceDirect

Chemical Geology

journal homepage: www.elsevier.com/locate/chemgeo

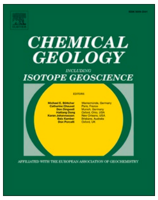

Determining static reservoir connectivity using noble gases

J.A. Scott [a,*], M. Pujol [b], D. Györe [c], F.M. Stuart [c], S.M.V. Gilfillan [a]

[a] School of GeoSciences, The University of Edinburgh, Grant Institute, James Hutton Road, Edinburgh EH9 3FE, UK
[b] Exploration and Production, TotalEnergies, CSTJF, Avenue Larribau, 64000-Pau, France
[c] Isotope Geosciences Unit, Scottish Universities Environmental Research Centre, Rankine Avenue, East Kilbride G75 0QF, UK

ARTICLE INFO

Editor: Don Porcelli

Keywords:
Noble gas
Fingerprinting
Geochemical tracing
Reservoir connectivity
Tormore
Gas connectivity
Oil connectivity
Vertical connectivity
Lateral connectivity

ABSTRACT

Determining the connectivity of fluids in hydrocarbon reservoirs is a key challenge during the appraisal stage. Such information is critical for assessing the economic viability and planning reservoir development. Although several tools exist to determine static connectivity and the fluid column organisation post-hydrocarbon emplacement, it is extremely difficult to determine the extent of the connectivity between fluids of different phases. Conventional connectivity studies on the Tormore field, West of Shetland Basin, UK have resolved the vertical connectivity of one well (T2) but have been unable to resolve further vertical or lateral connectivity. Here, we outline a new tool for assessing hydrocarbon connectivity by completing the first intra-field connectivity study of the noble gas composition (He, Ne, Ar, Kr and Xe) of fluids from individual reservoir units, allowing the resolution of both the vertical and lateral connectivity within the Tormore field. To achieve this, we obtain fluid samples from archived PVT vessels rather than from the wellhead or platform separators, allowing sampling of the individual reservoir units encountered during drilling. Our findings corroborate previous connectivity studies undertaken on the oil well, T2, confirming that the reservoir unit of T2-A is isolated from the lower reservoir units. We apply the same method to the gas well, T3, finding that unit T3-A is isolated from the lower reservoir units. In addition, we identify a previously unknown connection between the gas and oil phase that is separated by a poorly constrained fault. These findings confirm the effectiveness of using noble gas fingerprints to assess the connectivity of fluids in different phases, providing a new tool for understanding connectivity in hydrocarbon and non-hydrocarbon settings (e.g. Carbon, Capture and Storage).

1. Introduction

1.1. Introduction to connectivity

Determining the connectivity of hydrocarbon fluids within a reservoir is a crucial component of the appraisal stage of a field. Whilst definitive data to quantify fluid connectivity are generated once the reservoir enters the production phase, it is extremely difficult to obtain this data during the appraisal phase when critical decisions on the viability of the reservoir need to be taken. Many methods have been developed to assess the connectivity of a reservoir prior to production (e.g. Jolley et al., 2010 and papers within; Elshahawi et al., 2008) but rarely can all potential scenarios be fully resolved. Furthermore, it is currently particularly difficult to assess the connectivity between fluids of different phases.

This study investigates the interaction of fluids (connectivity or continuity) instead of barriers to fluid flow (compartmentalization). Connectivity is defined as the exchange of atoms, molecules or fluids between two bodies. Connectivity within a field varies on timescales ranging from the geological scale (>10,000 years) and production lifetime (<40 years) (Snedden et al., 2007). These are defined as static and dynamic connectivity, respectively.

Static connectivity describes the state of the field prior to production, whereas dynamic connectivity describes the movement of fluids once production has commenced (Snedden et al., 2007). It is also important to define the direction of connectivity in the vertical and lateral sense. Vertical connectivity is the communication of different reservoir units at varying depths within the same panel or fault block. Lateral connectivity is the communication within the same reservoir unit or across a physical discontinuity, e.g. a fault.

Poorly constrained connectivity has a profound and detrimental effect on hydrocarbon recovery; therefore, it is essential to resolve reservoir connectivity as early and as completely as possible during the exploration phase (Smalley and Muggeridge, 2010). 3D seismic, well

---

* Corresponding author at: Total, CSTFJ, Avenue Larribau, 64000 Pau, France.
E-mail address: james-alexander.scott@totalenergies.com (J.A. Scott).

https://doi.org/10.1016/j.chemgeo.2021.120410
Received 8 July 2020; Received in revised form 7 May 2021; Accepted 26 June 2021

logs and core analysis provide invaluable data and images over a large area during the exploration phase, allowing the identification of compartmentalization. However, these indirect methods cannot provide direct evidence or predict fluid behaviour.

There are three main conventional tools used to assess fluid connectivity of a hydrocarbon reservoir: drill stem test (DST) and formation testing; organic geochemistry; and thermodynamic modelling (Table 1). A DST is the first opportunity to directly investigate the connectivity of a field during the exploration/appraisal phase. This technique permits analysis of accumulating pressure in the well and pressure changes in nearby wells (i.e. an interference test). This can be used to provide an estimate of the reservoir volume and the likely connectivity can be resolved to a kilometre scale.

Formation testers, e.g. a Wireline Formation Tester (WFT), are downhole tools that sample reservoir fluids and record the pressure from each reservoir unit. If the pressure for each reservoir unit does not follow a common or resolvable pressure gradient, then the units are likely to be disconnected. However, the opposite is not true, i.e. if samples from the same phase follow a gradient, this is not conclusive evidence for a connection between the reservoir units.

Several conventional methods exist for the geochemical analysis and comparison of fluids. There are two main fields, qualitative, e.g. comparing and contrasting the organic geochemistry of the hydrocarbon fluid (e.g. Sammons maps) and quantitative, e.g. investigating the statistical significance of differences in hydrocarbon composition (e.g. Inter-Quartile Range treatment (IQR treatment)). These methods follow the same logic as many geochemical tools, where selected compounds are used to highlight differences or similarities within samples. However, both methods have their limitations for assessing connectivity as they focus on C_7 – C_{20} molecules. As a result of the wide range of hydrocarbon molecules required this method is only applicable to the liquid phase. When this method is applied to a gas phase there is insufficient liquid fraction available to sample, thus, any analysis is often below the significance threshold and is therefore inconclusive.

1.2. The rationale for noble gases

The noble gases (He, Ne, Ar, Kr and Xe) are present in trace quantities in all crustal fluids. They do not react with or degrade within hydrocarbon reservoirs in the same manner as organic tracers and hence provide ideal tracers of fluid interaction. Their distribution in crustal fluids is the result of physical interactions between different fluid sources and phases (Ballentine et al., 1991; Pinti and Marty, 1995; Kipfer et al., 2002; Burnard, 2013; Prinzhofer, 2013). Consequently, noble gases can be used to interpret the physical processes that are poorly constrained by reactive tracers.

In this study, we mainly focus on the atmosphere-derived noble gases (^{20}Ne, ^{36}Ar, ^{84}Kr and ^{132}Xe). These noble gases enter the meteoric water cycle during gas partitioning between the atmosphere and the surface of a large body of water e.g. an ocean. When these waters enter the subsurface either through aquifer recharge, pore trapping and/or wet sediment burial, an atmosphere-derived noble gas signature is imparted in the subsurface. Post-burial there is no other significant source of atmospheric noble gas in the subsurface. The trapped water is no longer able to exchange material with the overlying body of water, and therefore, the groundwater is isolated. Once isolated, the atmosphere-derived noble gas composition is unaffected by mixing with other waters or interacting with other fluids. Two other sources of noble gas exist in the subsurface (mantle and crustal), however, these bear no effect as they are devoid of atmosphere-derived isotopes. In petroleum systems, groundwater (e.g. an underlying aquifer) is rarely sampled or not encountered, hence, the groundwater composition is often unknown. Due to the unreactive nature of noble gases, it is possible to calculate the groundwater composition. Gas-specific Henry coefficients are assumed to depend on the temperature and salinity of the water (Fanale and Cannon, 1971; Crovetto et al., 1982; Castro et al., 1998; Kipfer et al., 2002). Therefore, the key control of atmosphere-derived noble gas signature in the subsurface is the temperature and salinity at the point of equilibrium (König et al., 1964 and Weiss, 1970). Thus, the equilibrium conditions at the point of recharge control groundwater composition. This unambiguous origin of atmosphere-derived noble gases provides great utility for understanding subsurface process e.g. assessing

Table 1

Limitations of the conventional methods for assessing reservoir connectivity. During the exploration phase, this is limited to indirect methods for identifying potential compartments or baffles to flow i.e. a fault. Post-drilling, more detailed analysis can be applied using reservoir data and fluids. However, these current methods have their limitations. It is currently difficult to determine the connectivity between the oil and gas phase at a scale of less than 1 km. In addition, we add the application of noble gases (grey).

		Method/Tool	Scale of resolution	Evidence of connection or disconnection	Applicable to a gas phase?	Applicable to an oil phase?	Applicable to a two-phase system?
Conventional methods	Exploration phase	3D Seismic	Intra-field (limited to ~50m)	Indirectly, identifying possibly physical discontinuities e.g. a fault	No	No	No
		Well Logs	Borehole	Indirectly	No	No	No
		Rock Core	Borehole	Indirectly	No	No	No
	Appraisal phase	Drill Stem Test (DST)	>1 km	Estimates connected volume	Yes	Yes	Yes
		Pressure test	Intra-field	Disconnection only	Yes	Yes	Yes
		Organic Geochemistry	Intra-field	Both	No	Yes	No
		Thermodynamic modelling (PVT)	Intra-field	Both	No	Yes	No
Our method		Noble gases	Intra-field	Both	Yes	Yes	Yes

hydrocarbon migration, storage and connectivity.

Previous noble gas studies have focussed on basin-wide and inter-field scale fluid migration, allowing the source, the degree of mixing between hydrocarbons and aqueous fluids isolation time, be determined (Zaikowski and Spangler, 1990; Hiyagon and Kennedy, 1992; Ballentine et al., 1996, 2002; Torgersen et al., 2004; Barry et al., 2016, 2017, 2018a,; Byrne et al., 2018, 2020). Other work has explored the interaction of natural CO_2 with formation waters (Gilfillan et al., 2008, 2009, 2014) along with tracing the fate of CO_2 in response to injection for enhanced oil recovery (Györe et al., 2015, 2017; Barry et al., 2018b; Tyne et al., 2019) and for the identification of compartmentalization in ancient fracture networks (Warr et al., 2018). However, to date noble gases have not been specifically applied for the assessment of intra-field connectivity between individual wells and reservoir compartments.

The principle of using noble gases for assessing reservoir connectivity follows the same logic as many conventional industry tools. Given time, a well-connected reservoir will reach a steady-state equilibrium with a predictable distribution of noble gases across a reservoir. Therefore, we can assume that spatially varying fluid related properties are good indicators of disconnection (Smalley and Muggeridge, 2010). When results diverge from the predicted distribution, this identifies an additional process such as flow retardation along a fault or baffle, or the influence of a recent external processes such as gas leakage (Montel et al., 1993). Such features and mechanisms can delay or perturb the return to steady-state conditions (Kaufman et al., 1990; Elshahawi et al., 2005). When considering reservoir connectivity, a reservoir unit that is disconnected may have a distinctive noble gas fingerprint due to their isolation (Hunt et al., 2012; Darrah et al., 2014, 2015). If the reservoir units are connected and in communication, then a resolvable distribution of noble gases across the field can be observed.

In this study, we use noble gas ratios as unique fingerprints of each reservoir unit to assess the source and physical processes that have acted upon the fluids, which in turn can show evidence of disconnection and connection. We recognise three distinct fingerprints for noble gases: 1) Primordial, sourced from the mantle, entrained during the Earth's accretion (Oxburgh et al., 1986; O'Nions and Oxburgh, 1988; Honda et al., 1991; Burnard et al., 1997; Graham, 2002). 2) The crustal component, inherited from the hydrocarbon source rock and the in situ radiogenic and nucleogenic generation in the reservoir (^{4}He & ^{40}Ar) or from migration through an aged aquifer to the trap (Morrison and Pine, 1955; Sarda et al., 1988; Kennedy et al., 1990; Moreira and Allègre, 1998; Ballentine and Burnard, 2002). 3) The primordial aquifer component, an atmosphere-derived component which enters the subsurface via aquifer recharge and/or entrained in the original formation water of the sediment (Kipfer et al., 2002). Initial fingerprints can be altered by physical processes such as diffusive fractionation (e.g. Prinzhofer and Battani, 2003) related to hydrocarbon migration distance, leakage of fluids from or on-going charging of the field (e.g. Battani et al., 2000; Barry et al., 2016) and by equilibration within the reservoir, e.g. the exchange of noble gases at the water-oil contact (OWC) (Fig. 1).

Here we present new noble gas isotope and abundance data from the Tormore field, West of Shetland basin. The Tormore field is a diphasic system where conventional methods for assessing reservoir connectivity have failed to confidently resolve the connectivity of the field, particularly between the oil and gas phases, making it an ideal candidate for investigating the role that noble gases can play in assessing connectivity. Fluid samples were collected downhole directly from individual reservoir units, permitting a detailed study of the role that noble gases can play in establishing reservoir connectivity.

2. Geological background

2.1. The West of Shetland Basin

The Faroe-Shetland Basin is situated in the north-eastern part of the North Atlantic margin. Bound by the Wyville-Thomson ridge to the south-west; the Nordland-Silje transfer fault in the north-east; and the Shetland Platform to the south-east. Mesozoic extension created the accommodation space for thick sedimentary sequences within the basin and the majority of the West of Shetland ridges: Shetland Platform, Corona, Rona and Flett Ridge (Naylor et al., 1999).

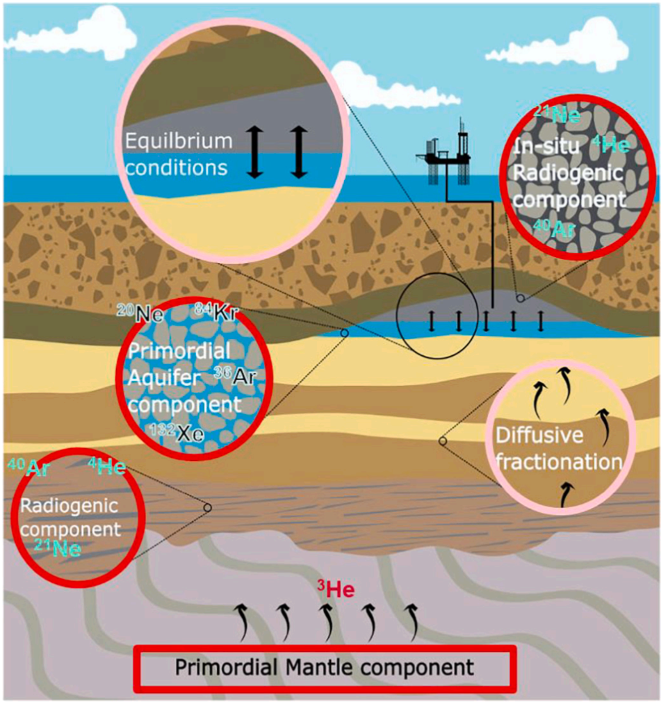

Fig. 1. Cartoon illustrating the main controls on noble gas fingerprints within a hydrocarbon system. There are three sources of noble gases (red): 1) Primordial, sourced from the mantle, and entrained during the Earth's accretion 2) The crustal component from nucleogenic production and radiogenic decay of U, Th and K. 3) Primordial aquifer component enters the subsurface via aquifer recharge and/or entrained in the original formation water of the sediment. In addition, there are two main physical controls on noble gases within a petroleum system (pink); (i) diffusive fractionation and (ii) the solubility-controlled exchange of noble gases between the aquifer and the trapped hydrocarbon fluids. (For interpretation of the references to colour in this figure legend, the reader is referred to the web version of this article.)

The Early Paleocene c.62 Ma marks the onset of seafloor spreading in the NE Atlantic and the opening of the Faroe-Shetland Basin (White and McKenzie, 1989). Extension continued up to and during the Paleocene. During the Eocene, a basin-wide regional uplift and inversion event is attributed to creating the structural traps for many petroleum plays within the basin. The observed inversion and uplift are interpreted as the result of plume buoyancy, magmatic under-plating or a combination of both (Brodie and White, 1994). This event is well marked in Paleogene stratigraphy through a series of regressive and transgressive depositional sequences across the basin.

Dolerite sill complexes and associated dykes were intruded in the Upper Cretaceous-Paleocene intervals. Radiometric analysis has dated the intrusions from the Late Cretaceous to Eocene in age (Ritchie and Hitchen, 1987; Naylor et al., 1999). These sill complexes are believed to be a key control of hydrocarbon migration across the Faroe-Shetland Basin (Iliffe et al., 1999).

2.2. The Tormore field

The Tormore field is located in Quadrant 205 (Fig. 2). Exploration of the basin has occurred for over 40 years but due to its complexity and isolation from infrastructure, appraisal and production from field discoveries has been limited until recently (Austin et al., 2014). The field is

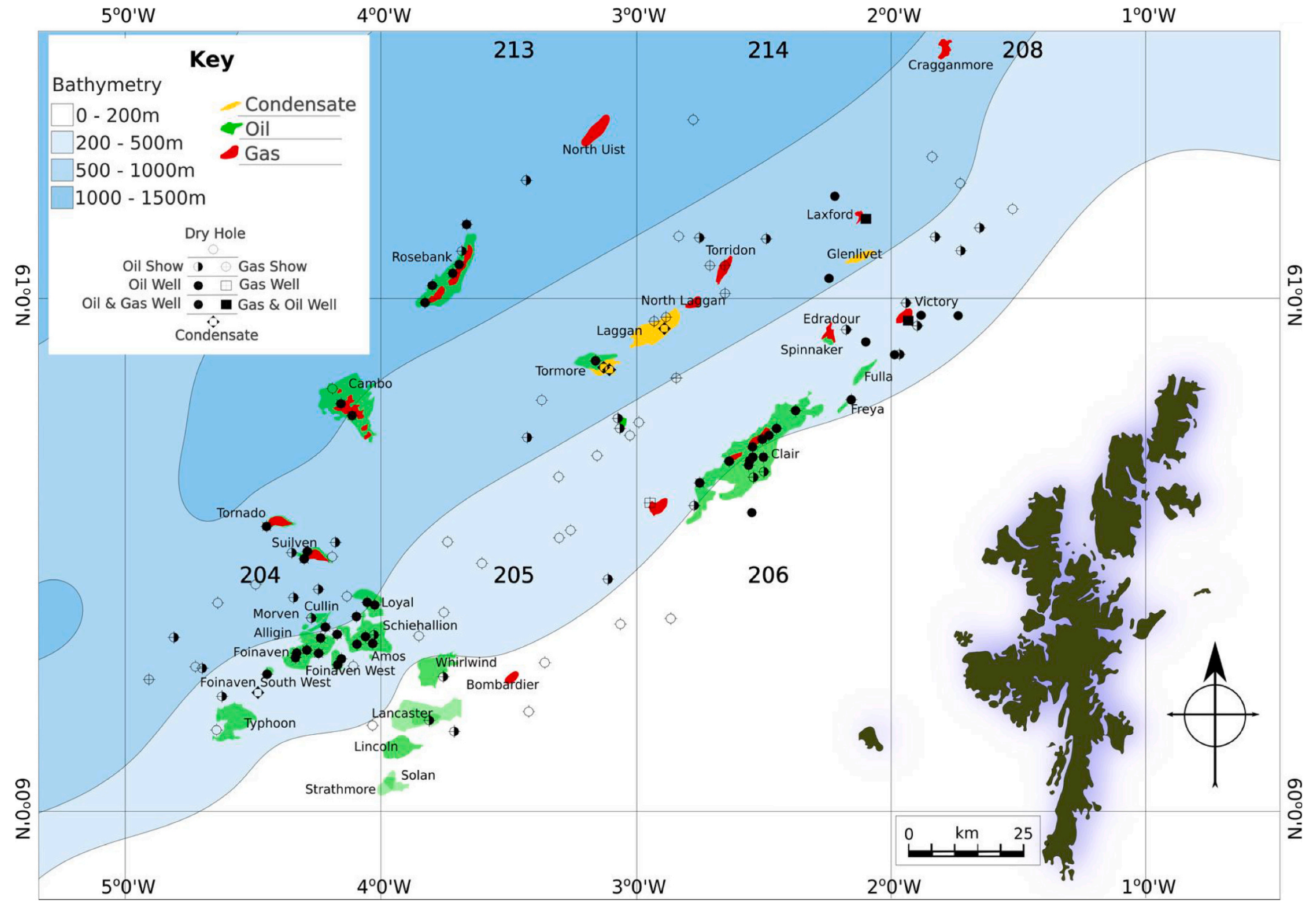

Fig. 2. Location map of the UK West of Shetland Basin. The Tormore field is located in a water depth of ~600 m, 140 km north-west of the Shetland Islands in Quadrant 205. The locations and closure of all petroleum fields in the exploration or appraisal phase are provided along with the bathymetry of the basin (Doré et al., 1997). Also shown are the locations of the completed wells in the WoS basin (taken from the UK Government Oil and Gas Authority, www.ogauthority.co.uk).

a simple monocline structure dipping to the northwest, on-lapping the Flett Ridge. The reservoir comprises of four reservoir units (A, B, C & D) of well-sorted Paleocene turbiditic sand exhibiting a high average porosity and permeability of 22% and 30–300 mD respectively. The individual reservoir units are separated by hemipelagic shale layers, with a total reservoir thickness of 50–60 m. Seismic studies have revealed a series of *E*-W antithetic normal faults throughout the field. A poorly constrained normal fault with an unknown transmissivity separates T2 and T1 wells (Fig. 3).

Three wells (T1, T2 and T3) have been drilled and completed since exploration commenced in 2006, using a water-based drilling fluid. To date, neither a gas-oil contact (GOC) nor water-oil contact (OWC) has been encountered. Well T2 encountered only oil and T1 and T3 penetrated gas-condensate. Studies by the field operator indicate that the field has been charged by two different fluids: initially, by a low-maturity dense fluid with a vitrinite reflectance equivalent (V_{re}) 0.8% Ro, followed by a second more mature, low-density fluid ($V_{re} \sim 1.2\%$ Ro). These fluid charges are well-mixed across the field and both V_{re} values are observed in both fluid phases. Therefore, the observed phases in the field are a result of Pressure, Volume and Temperature (PVT) conditions and not a reflection of the fields charging history. The field is a closed system with no evidence of leakage or spillage.

Conventional connectivity tools have enabled resolution of the vertical connectivity of T2. This investigation concluded that reservoir unit T2-A is isolated from T2-C and T2-D (Fig. 3) but no other conclusions could confidently be drawn for the vertical and lateral connectivity of the other wells or the remainder of the field.

3. Sample collection and analytical techniques

3.1. *Sampling from PVT vessels*

All reservoir fluids were collected downhole from the individual reservoir units during the drilling process using a Wireline Formation Tester (WFT). A WFT collects 400 cm^3 of virgin reservoir fluid under reservoir temperature and pressure (RTP) into a vacuum chamber after flushing the downhole sampling area of drilling fluid. These samples are then brought to the surface and stored onshore at reservoir pressure in conventional PVT sample storage vessels.

The specially constructed cells for collecting subsamples for noble gas analysis, comprised of Swagelok stainless steel cells (35 cm^3) sealed at each end with all-metal valves. Prior to being transported to the PVT vessel storage facility, each sampling cell was pre-evacuated to below 10^{-7} mbar, baked at 60 °C for 30 min and then helium leak tested. The cells were attached to the PVT vessel with a 0.25 cm^3 stainless steel pipe and the system was heated above 50 °C to minimise gas condensation. The sample cells were evacuated with a low vacuum pump to 10^{-2} to 10^{-3} mbar for 15 min. The valves on the sampling cell were then closed and the PVT vessel was equilibrated with the fluid in the connecting pipe for one minute. The PVT vessel was then isolated, and the connecting pipe then evacuated for 5 min. This process was repeated twice. For sample collection, the was PVT vessel equilibrated with fluid from the PVT vessel for 1 min then the cell was filled with reservoir fluid at 2–3 bar g.

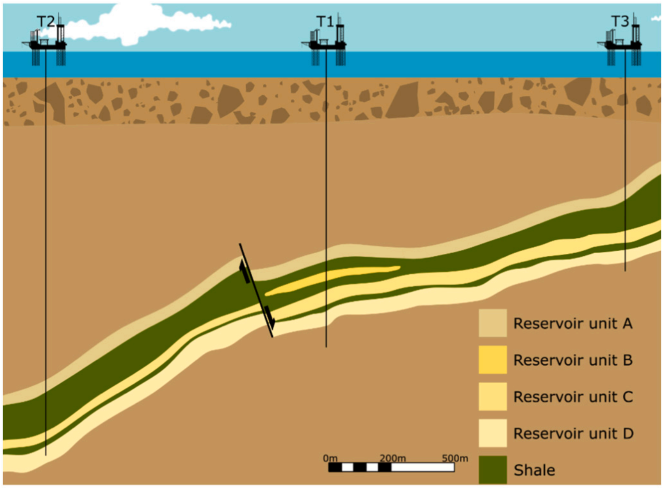

Fig. 3. Carton cross-section based on interpreted seismic data of the Tormore field. Three wells have been drilled; T1, T2 and T3. This study investigates the connectivity the reservoir units that lie within the Tormore field, namely reservoir units A, B, C & D the lateral extent of unit B is unknown. Separating each unit is a layer of hemipelagic shale (green) with a varying lateral thickness of 2-10 m. Wells T1 and T3 encountered gas-condensate, whilst T2 solely encountered oil. During the drilling and appraisal phase of the field, no water-oil contact or gas-oil contact was encountered. Separating T2 and T1 is an antithetic normal fault with an unknown offset and transmissibility. Figure is vertically not to scale. (For interpretation of the references to colour in this figure legend, the reader is referred to the web version of this article.)

3.2. Major volatile analysis

Methane and ethane compositions were determined using extended gas chromatography using a GPA 2286 method utilising a multicolumn gas chromatograph system at Total's laboratory following ISO 140001 and ISO 7000 compliant procedures.

3.3. Noble gas analysis

Noble gas analysis was conducted at the Scottish Universities Environmental Research Centre (SUERC) using a MAP 215–50 noble gas mass spectrometer. Helium, neon and argon concentration and isotopic ratios were obtained using the procedures outlined by Györe et al. (2015) and Kr and Xe were measured following procedures documented in Györe et al. (2017).

4. Results

Nine reservoir units from three wells were sampled, resulting in the collection of 12 samples (including 3 duplicates in T3). The reservoir interval sampled, well depth, natural gas data (C_1, C_2 and $\delta^{13}C_{1–5}$ abundance), noble gas abundance and isotopic composition measurements are documented in Tables 2–4. Reservoir units T2-B, T3-B and T1-A were not sampled during the exploration drilling operations.

4.1. Major volatiles and isotopic data

In the gas-condensate wells, T1 and T3, the major gases are dominantly hydrocarbons C_1 (86.6–87.3%); C_2 (3.8–4.0%) (Table 3). C_1/C_2 ratios are similar across both wells (21.8–23.2), demonstrating that there is no leakage from the top of the field (Montel et al., 1993). Isotopic values are broadly similar in the gas-condensate wells where, $\delta^{13}CH_4$ (−37.3 to −37.6), $\delta^{13}C_2H_6$ (−30.9 to −31.1), $\delta^{13}C_3H_8$ (−29.5 to −29.7), $\delta^{13}C_4H_{10}$ (−28.3 to −29.23) and $\delta^{13}C_5H_{12}$ (−27.4 to −28.1) (Table 4). For the oil well, T2, the major gases comprised of hydrocarbons C_1 (62.2–62.8%); C_2 (4.0–4.4%) (Table 3). For T2, the isotopic values are more negative than those in the gas phase $\delta^{13}CH_4$ (−38.1 to −38.3), $\delta^{13}C_2H_6$ (−30.7 to −31.1), $\delta^{13}C_3H8$ (−29.2 to −29.9, $\delta^{13}C_4H_{10}$ (−27.8 to −28.0) and $\delta^{13}C_5H_{12}$ (−27.5 to −27.6) (Table 4).

4.2. Noble gases

$^4He/^{20}Ne$ ratios of all reservoir units range from 0.49 to 5525 (Table 3), with all but one sample (T1-B) being significantly above the air ratio of 0.32 and air-saturated seawater (ASSW) ratio of 0.252 (Kipfer et al., 2002). There is a low in situ production of ^4He due to low U and Th concentrations in the reservoir sandstones due to their low clay content. The elevated $^4He/^{20}Ne$ ratios indicate that the atmospheric contributions in all samples are negligible with the exception of T1-B.

Helium (^4He) concentrations range from 6.08×10^{-6} to 5.21×10^{-5} cm^3 STP/cm^3. $^3He/^4He$ values range from 0.051 ± 0.003 to 0.367 ± 0.034 R/R_A (relative to the air value $R_A = 1.384 \times 10^{-6}$, where air = 1 R/R_A; Mamyrin et al., 1970). These are resolvable excesses of crustal production and requires a contribution of mantle helium (Ballentine et al., 2002). Using simple two-component mixing between sub-continental lithospheric mantle-like (6.1 R_A (Gautheron and Moreira, 2002)) and crustal (0.007–0.02 R_A) endmembers (Ballentine and Burnard, 2002; Day et al., 2015) indicates that crustal contribution to the ^4He concentration varies from 91.2 to 97.6%.

^{20}Ne concentrations range from 5.81×10^{-9} to 4.26×10^{-8} cm^3 STP/cm^3. There is a clear correlation between ^{20}Ne concentrations and proximity to the predicted oil-water contact, where ^{20}Ne increases with depth (Table 2). $^{20}Ne/^{22}Ne$ vary between 9.65 ± 0.036 and 9.86 ± 0.039

Table 2

Concentrations of non-radiogenic noble gas isotopes, reservoir unit and sampling depth in the Tormore field. Noble gas concentrations are given to three significant figures under STP conditions in cm^3 STP/cm^3. Depth is True Vertical Depth sub-sea (TVDss) in meters. Air values are after Ozima and Podosek (2002) and ASSW value are after (Kipfer et al., 2002).

Well	Reservoir Unit	Depth (TVDSS m)	^{20}Ne	1σ	^{36}Ar	1σ	^{84}Kr	1σ	^{132}Xe	1σ
T1	B	3755	1.50E-05	6.38E-07	1.79E-05	6.65E-07	7.01E-07	2.91E-08	2.23E-08	1.17E-09
	C	3767	1.06E-08	4.51E-10	5.48E-08	2.06E-09	2.38E-09	9.90E-11	3.35E-10	1.75E-11
	D	3777	2.03E-08	8.65E-10	1.61E-07	6.01E-09	5.91E-10	2.46E-11	1.03E-10	5.38E-12
T2	A	3831	4.26E-08	1.81E-09	1.25E-07	4.64E-09	4.15E-09	1.73E-10	4.15E-10	2.17E-11
	C	3878	1.28E-08	5.48E-10	6.21E-08	2.34E-09	2.52E-09	1.05E-10	3.60E-10	1.89E-11
	D	3888	2.07E-08	8.77E-10	7.58E-08	2.86E-09	2.96E-09	1.23E-10	3.64E-10	1.91E-11
T3	A	3670	5.90E-09	3.54E-10	3.62E-08	1.37E-09	1.70E-09	7.07E-11	3.06E-10	1.04E-11
	Duplicate		8.50E-09	2.47E-10	3.96E-08	1.53E-09	2.00E-09	4.14E-11	3.10E-10	1.60E-11
	C	3700	7.69E-09	3.26E-10	4.09E-08	1.53E-09	2.11E-09	8.76E-11	2.74E-10	1.43E-11
	Duplicate		7.31E-09	3.10E-10	4.29E-08	1.59E-09	2.10E-09	8.73E-11	3.02E-10	1.58E-11
	D	3706	6.78E-09	8.88E-11	4.03E-08	6.81E-10	2.15E-09	9.13E-11	3.34E-10	9.58E-12
	Duplicate		1.15E-08	1.83E-10	4.13E-08	7.03E-10	1.96E-09	8.34E-11	2.75E-10	7.91E-12
Air			1.65E-05		3.14E-05		6.50E-07		3.54E-09	
ASSW at 4 °C			1.55E-07		1.16E-06		4.74E-08		4.31E-09	

Table 3
Radiogenic noble gas abundances and ratios in the Tormore field. Concentrations are given to three significant figures in standard conditions are after Ozima and Podosek (2002) in cm^3 STP/cm^3. Air composition is after Eberhardt et al., 1965; Honda et al., 2015; Mamyrin et al., 1970; Mark et al., 2011; Ozima and Podosek (2002).

Well	Reservoir Unit	C_1%	C_2%	$^3He/^4He$ (R/R_a)	1σ	^4He	1σ	$^{20}Ne/^{22}Ne$	1σ	$^{21}Ne/^{22}Ne$	1σ	$^{40}Ar/^{36}Ar$	1σ	$^4He/^{20}Ne$	1σ
T1	B	88.6	3.95	4.45E-01	2.73E-02	7.30E-06	3.73E-07	9.65	0.08	2.87E-02	5.04E-04	300	1	0.49	0.04
	C	86.7	3.81	1.95E-01	9.54E-03	4.40E-06	4.61E-09	9.67	0.08	3.09E-02	5.20E-04	537.19	3	414	27
	D	86.8	3.82	2.14E-01	1.32E-02	2.20E-06	1.13E-07	9.81	0.09	2.94E-02	5.49E-04	464.63	2	108	8
T2	A	62.2	4.05	1.53E-01	9.40E-03	8.20E-06	4.19E-07	9.8	0.08	2.92E-02	5.10E-04	397.88	2	193	14
	C	62.5	4.41	5.09E-02	3.13E-03	1.60E-05	8.17E-07	9.84	0.09	2.99E-02	5.40E-04	509.13	4	1246	93
	D	62.8	4.36	1.65E-01	1.02E-02	8.40E-06	4.28E-07	9.54	0.08	2.96E-02	4.89E-04	445.99	3	407	30
T3	A	91.7	3.92	2.70E-01	1.30E-02	3.26E-05	1.20E-06	9.81	0.04	3.14E-02	3.46E-04	586.73	4	4447	276
	Duplicate			2.60E-01	1.20E-02	3.78E-05	1.20E-06	9.83	0.04	3.12E-02	3.78E-04	548.13	6	5525	352
	C	92.1	3.82	2.56E-01	1.12E-02	3.73E-05	1.91E-06	9.67	0.04	3.11E-02	3.66E-04	566.41	3	4851	295
	Duplicate			2.57E-01	1.41E-02	3.58E-05	1.83E-06	9.71	0.04	3.12E-02	3.38E-04	573.02	2	4898	339
	D	92.3	3.75	2.69E-01	3.86E-03	3.08E-05	9.10E-07	9.78	0.04	3.14E-02	3.46E-04	555.88	3	4549	88
	Duplicate			2.69E-01	4.12E-03	2.98E-05	8.80E-07	9.86	0.04	3.06E-02	2.57E-04	549.14	3	2603	57
Air				1		5.24E-07		9.81		2.90E-02		298.6		0.31	

Table 4
Carbon isotopic values for C_1 to C_5 from the three wells of Tormore. Values are reported in per mil ‰.

Well	Reservoir unit	C_1H_4 (±0.4‰)	C_2H_6 (±0.4‰)	C_3H_8 (±0.4‰)	C_4H_{10} (±0.4‰)	C_5H_{12} (±0.4‰)
T1	C	−37.6	−30.9	−29.4	−28.3	−27.9
T2	A	−38.3	−30.7	−29.2	−28.0	−27.6
	C	−38.1	−31.1	−28.9	−27.8	−27.5
	D	−38.1	−31.1	−29.2	−27.9	−27.5
T3	A	−37.3	−31.1	−29.7	−29.7	−28.1
	C	−37.3	−31.1	−29.7	−28.3	−28.0
	D	−37.3	−31.3	−29.9	−28.4	−28.0

indicating little deviation from atmospheric ^{20}Ne /^{22}Ne (9.80). $^{21}Ne/^{22}Ne$ ratios vary between 0.0296 ± 0.0005 and 0.0319 ± 0.0004, all in excess of the atmospheric value of 0.0290 (Eberhardt et al., 1965), this excess can be explained by an addition of crustal radiogenic ^{21}Ne to air-like neon.

^{40}Ar concentrations range from 2.12 to 4.96 × 10^{-5} cm^3 STP/cm^3. $^{40}Ar/^{36}Ar$ range from 398 ± 2 to 587 ± 4, indicating a significant deviation from the atmospheric $^{40}Ar/^{36}Ar$ value of 298.56 (Lee et al., 2006) due to a resolvable contribution of radiogenic ^{40}Ar. $^{38}Ar/^{36}Ar$ values vary between 0.186 ± 0.007 to 0.190 ± 0.004 which overlap with the air ratio of 0.1885 (Lee et al., 2006).

^{84}Kr and ^{132}Xe concentrations range from 4.15 × 10^{-9} to 9.95 × 10^{-10} cm^3 STP/cm^3 and 1.98 × 10^{-10} to 4.15 × 10^{-10} cm^3 STP/cm^3, respectively. $^{132}Xe/^{84}Kr$ ratios range from 0.03 to 0.18, with most samples ranging between 0.10 and 0.18, significantly above both the air (0.03) and ASSW ratios (0.09) (Kipfer et al., 2002).

4.3. *Groundwater noble gas components*

In this study ASSW is defined as a seawater which has equilibrated with air at 4 °C (following Kipfer et al., 2002). Water-derived noble gases for $^{20}Ne/^{36}Ar$ range from 0.1260 ± 0.007 to 0.3417 ± 0.038, $^{84}Kr/^{36}Ar$ 3.66 × 10^{-3} to 5.32 × 10^{-2} and $^{132}Xe/^{36}Ar$ 3.33 × 10^{-3} to 8.28 × 10^{-3}.

Krypton and xenon in the majority of samples correlates with ^{36}Ar and ^{20}Ne showing clear increase with depth (Tables 2 & 3). This confirms that the main source of ^{84}Kr and ^{132}Xe in the Tormore field is from the dissolved air-component present within the groundwater.

5. Discussion

5.1. *Assessing sample quality and sampling procedure*

PVT vessels are widely used in the hydrocarbon industry for preserving fluid at reservoir pressures in excess of 1000 bar for up to 10 years. Hence, the high-pressure sealing valves of PVT vessels can be expected to be sufficiently sealed to preserve the integrity of samples for noble gases over a prolonged period.

The standard method for collecting samples for noble gas analysis is purging stainless steel cylinders or refrigeration grade copper tubes at the wellhead (e.g. Holland and Gilfillan, 2013) or from platform gas separators (Ballentine et al., 1996). In this study, we use samples collected from boreholes at depths of 3700–4000 m TVDss, directly sampling from the reservoir unit and providing a specific depth. This method allows collection of a sample from each individual reservoir unit, allowing a noble gas fingerprint for each unit to be obtained. Thus, providing a greater depth resolution compared to samples collected at the wellhead. However, only a finite volume of reservoir fluid can be collected on the drill string (typically 400 cm^3 per canister). This means it is not possible to use prolonged purging procedures to ensure there is no contamination. As this is the first study to obtain noble gas samples from such vessels, we investigate the integrity of the samples to atmospheric contamination.

The majority of samples (n = 10), have relatively consistent noble gas concentrations, though we observe two outlier samples (T1-B and T1-D) (Tables 3.2 & 3.3). With the exception of T1-B, $^4He/^{20}Ne$ ratios (108 to 5525), demonstrating that atmospheric neon contributions in all but one of the samples is negligible.

In Fig. 4, $^{20}Ne/^{36}Ar$ is plotted against $^{21}Ne/^{22}Ne$, highlighting that

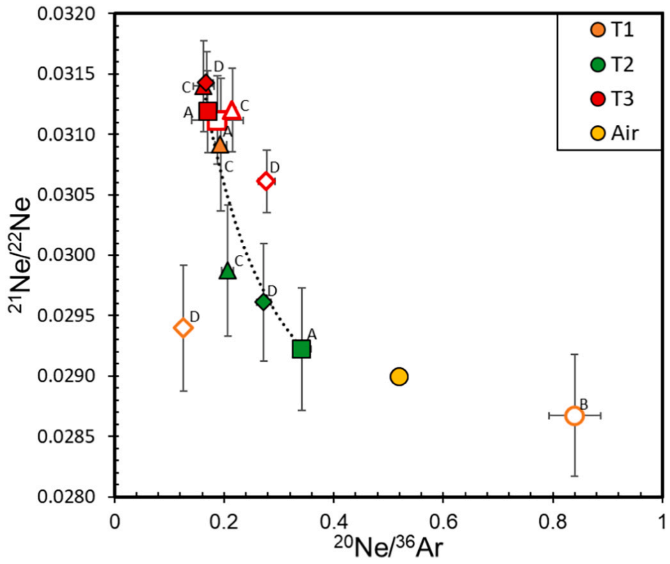

Fig. 4. Plot of ^{20}Ne/36Ar against ^{21}Ne/^{22}Ne of all samples from Tormore. Across the Tormore field, there is a clear mixing trend between T3-D and T2- A. Samples (T1-B and T1-D) show a clear deviation from this trend. These samples exhibit low ^{4}He/^{20}Ne ratios, indicative of a high atmospheric air contribution. Hence, these samples are omitted from further discussion. In the remaining samples, we observe a clear geographical trend. Samples from both of the wells that encountered gas condensate - T1 (orange) and T3 (red), located near the top of the structure show an elevated radiogenic component relative to the oil well T2 (green). This well targets the lower section of the field and exhibits a strong influence from an aquifer-derived atmospheric component. Uncertainties are 1 σ. (For interpretation of the references to colour in this figure legend, the reader is referred to the web version of this article.)

the samples with the most nucleogenic neon isotope ratios also exhibit the lowest ^{20}Ne/^{36}Ar. We observe a mixing relationship between the most radiogenic sample, T3-D and the least radiogenic T2-A. Two samples (T1-B and T1-D) clearly deviate from this trend. For T1-D, the lighter noble gases (He, Ne) are consistent with the majority of samples, once a small addition of atmospheric air is accounted for. However, this is not the case for the Ar and Kr, where we observe a magnitude lower measured ^{84}Kr compared to other samples and elevated ^{36}Ar, suggesting an addition of atmospheric air (Table 2).

Whilst samples T1-B and T1-D were collected from the same well, there is no trend to the data that indicates the fractionation observed is a geographically distinct feature. It is more likely that it is linked to the storage in PVT vessels for the 8 years prior to sampling for noble gas analysis. Hence, we exclude both from further interpretation.

Obtaining a sample at 2–3 bar in the sampling cell from a PVT vessel at reservoir pressure can result in mass-dependent fractionation, resulting in a loss of the lighter noble gases during each purge or flush. To assess the reliability of the sampling procedure, we examine the duplicates collected from each PVT vessel for Well T3.

In Fig. 5, we plot ^{20}Ne/^{22}Ne against ^{21}Ne/^{22}Ne, which illustrates clear repeatability between the first sample collected (solid red marker) and the duplicate sample (red outline marker). Samples from T3-A and T3-C are within 1 σ standard deviation in both ^{20}Ne/^{22}Ne and ^{21}Ne/^{22}Ne ratios. For T3-D, we observe an agreement in ^{20}Ne/^{22}Ne between the first sample collected and the duplicate, but not in ^{21}Ne/^{22}Ne. The cause of this is unknown but is potentially related to the smaller volume of fluid (~250 cm^{3}) in the PVT vessel compared to the larger 400 cm^{3} volume of the other PVT vessel sampled. Given the reproducibility of the results from the duplicate samples, we conclude that we have obtained reliable noble gas samples from PVT vessels and are not fractionating the noble gases during the flushing process.

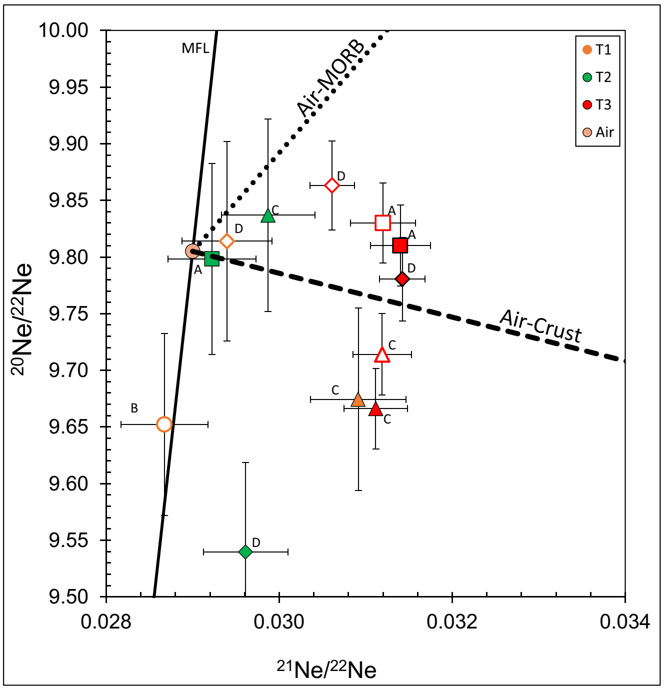

Fig. 5. Neon isotope plot of the Tormore field. Data presented are samples from all three wells. Outlier samples and duplicates (white) have a coloured outline corresponding to the well and the marker type reflects the reservoir unit. We observe a clear difference between samples from the oil phase (T2) and gas phase (T1 and T3). Samples from T2 plot near to the air-value, whereas samples from T3 plot along the air-crust line and exhibit a degree of mass fractionation away from the air-crust line. MFL is the mass fractionation line. Uncertainties are 1 σ.

5.1.1. *Quantifying the amount of air in the samples*

^{20}Ne is mainly concentrated in the air (typically 3–4 orders of magnitude higher in concentration than encountered in the subsurface). Hence, it is an ideal indicator for atmospheric air contamination in samples. In this study, we identify three endmembers within our samples. Two are well-constrained, ASSW and atmospheric air (Ozima and Podosek, 2002) and a third, unknown endmember, representing the initial hydrocarbon signature. Though the initial composition is unknown, a theoretical limit for the noble gas composition in the hydrocarbons can be determined based on noble gases partition (Bosch and Mazor, 1988; Barry et al., 2016).

In Fig. 6, we plot ^{20}Ne against ^{20}Ne/^{36}Ar. Two mixing lines show the evolution between atmospheric air and ASSW (blue dashed line) and between atmospheric air and the theoretical noble gas composition in the hydrocarbon phase (red dashed line). The air - hydrocarbon mixing line is constrained using the measurements from well T3. These samples are the most recently sampled and the least concentrated in ^{20}Ne, and therefore, the least likely to be contaminated. Where the theoretical compositional limit and air-hydrocarbon mixing line intersect, we propose this as the hypothetical initial endmember of the hydrocarbon fluids. From this endmember we can quantify the percentage of atmospheric air contribution in our samples from T3 and allowing constraint of a minimal contribution of atmospheric air of 0.0002–0.0015%. When the same method is applied to wells T1 and T2 we are unable to resolve these differences solely by atmospheric air addition. Using the initial hydrocarbon endmember, we evoke tertiary mixing between the three endmembers. From this, we constrain that there is a dissolved air component (from the groundwater contained in the water leg in the reservoir) of 0.7–1.5% in the ASSW with an extraneous atmospheric air content of 0.0122–0.12% in samples from T1 and T2.

Comparing these extraneous air values with other studies, the samples collected from T3 contain 1–2 orders of magnitude less air

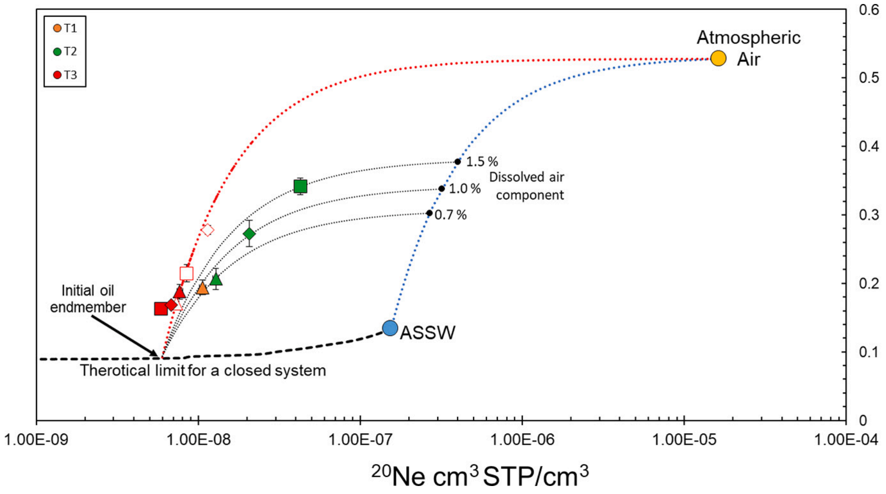

Fig. 6. Neon concentrations vs. $^{20}Ne/^{36}Ar$ with all samples that passed the initial quality control In the samples from the Tormore field, there are two well-constrained endmembers ASSW (blue marker) and atmospheric air (yellow marker) (Ozima and Podosek, 2002) and a third unknown endmember, the original hydrocarbon signature. A theoretical limit for the noble gas composition in the original hydrocarbon phase is determined for a closed system (Barry et al., 2016; Bosch and Mazor, 1988). In addition, two binary mixing lines show the mixing between atmospheric air and ASSW (blue dashed line) and between air and the theoretical noble gas composition in the hydrocarbon phase (red dashed line). Where, the compositional limit and air-hydrocarbon mixing line intersect, we propose this as the hypothetical endmember of the hydrocarbon fluids. (For interpretation of the references to colour in this figure legend, the reader is referred to the web version of this article.)

contamination than comparable studies (e.g. Barry et al., 2016, 2017). When this is compared to the older archived samples (T1 and T2), our method of sampling is within the same order of magnitude of previous work of Barry et al. (2016, 2017). Combining these findings with other noble gas ratios of the values of Tormore $^4He/^{20}Ne$ (413.94–5525.42), $^{40}Ar/^{36}Ar$ (398–587), and $^{132}Xe/^{84}Kr$ (0.10–0.18) there is a significant deviation from air values. We demonstrate that there is a measurable, but very small atmospheric air contribution in our samples. In addition, this confirms that our methods for collecting hydrocarbons samples directly from the reservoir and subsampling are robust for noble gas analysis.

5.1.2. *The source of atmospheric-derived noble gases in samples*

Atmosphere-derived noble gases are transported into the subsurface by water, either through aquifer recharge or within water-saturated pores as sediment is buried (e.g. Kipfer et al., 2002). The initial concentration of noble gases in the ground (or pore) water can be reasonably well constrained from solubility data and accounting for contributions from excess air (Crovetto et al., 1982; Wagner and Pruss, 1993; Harvey, 1996; Ballentine and Hall, 1999; Peeters et al., 2002; Fernández-Prini et al., 2003; Aeschbach-Hertig et al., 2008; Tolstikhin et al., 2017). The solubility of noble gases is controlled by atomic size, with heavier noble gases being considerably more soluble than the lighter elements (He < Ne < Ar < Kr < Xe). Using the solubility of noble gas in hydrocarbons and water, it is possible to model the partitioning behaviour for noble gases between water and hydrocarbons in the subsurface. These models typically assume that all atmospheric-derived noble gases are sourced from buried groundwater and all hydrocarbon fluids are devoid of these noble gases until they interact with the groundwater (Pujol et al., 2018).

The initial model outlined by Bosch and Mazor (1988) uses ratios of atmospheric-derived $^{20}Ne/^{36}Ar$, $^{84}Kr/^{36}Ar$ and $^{132}Xe/^{36}Ar$ to predict partitioning patterns in water-oil and water-gas systems. These models were later expanded and built upon by Battani et al. (2000); Zhou et al. (2005); Gilfillan et al. (2008) and Barry et al. (2016). These models represent a binary mixing between one phase e.g. gas, oil or CO_2 with water. However, the charging history of Tormore is not a simple binary mixing of two fluids and therefore these models are not appropriate models for the processes that have occurred with the field.

Hence, we apply Bosch and Mazor's (1988) model to the Tormore field that as this more accurately reflects the known history of double charging of hydrocarbons within the field. Fig. 7a shows the evolution of noble gases when an oil or a gas strips an aquifer of noble gases by a batch fractionation process. Noble gases have different solubilities in gas and oil, therefore when the first "droplet" of oil or "bubble" of gas passes through an aquifer, the individual noble gases will partition to different

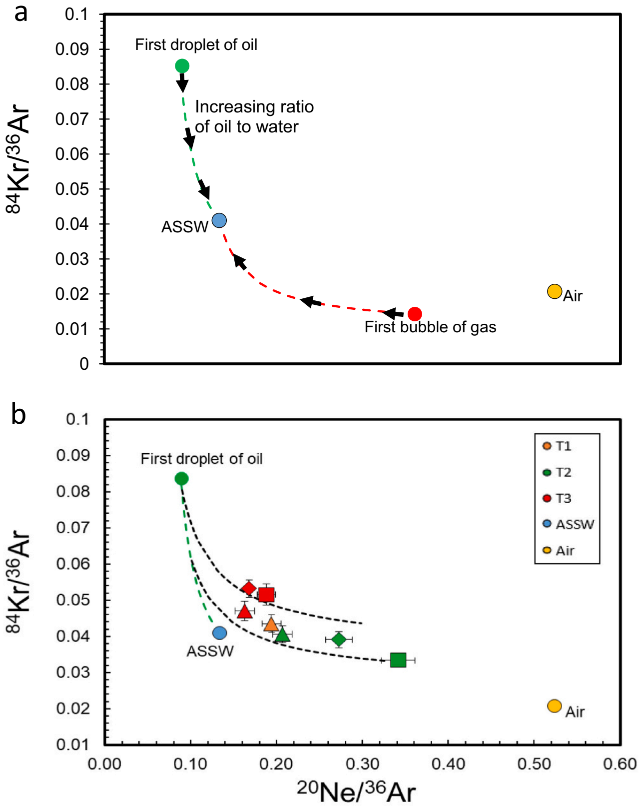

Fig. 7. Closed-system batch fractionation under the reservoir conditions of Tormore. a) Noble gas fingerprints will evolve differently when they interact with an oil or a gas. The green line shows the fractionation pattern of an oil and the red line represents a gas. The first droplet/ bubble represents an infinitesimally small volume of hydrocarbon fluid passing through an infinite aquifer. Given a large enough volume of hydrocarbons, the noble gases will fully partition in the hydrocarbons and inherit a noble gas fingerprint similar to that of the aquifer. b) Applying the known charging history of Tormore, we model a batch fractionation of a gas stripping oil and use the measured samples from Tormore to constrain an upper and lower limit. We find a Voil/Vwater of 0.003 to 0.06 for the Tormore. Uncertainties for measured noble gases are 1 σ. ASSW at 4 °C is after Kipfer et al. (2002) and air is after Ozima and Podosek (2002). (For interpretation of the references to colour in this figure legend, the reader is referred to the web version of this article.)

extents based on solubility (Crovetto et al., 1982; Wagner and Pruss, 1993; Harvey, 1996; Fernández-Prini et al., 2003). Theoretically, with an infinite hydrocarbon to water ratio within a closed system under ideal conditions, all noble gases will eventually partition into the hydrocarbon phase resulting in an ASSW-signature being transferred to the hydrocarbon phase.

Tormore was charged by two fluids with a common, the differences in fluid composition with depth i.e. gas condensate and oil are an effect of PVT conditions. The light carbon molecules are $C_1 – C_5$ are unaffected by phase changes, hence, we can directly compare the oil and gas-condensate in terms of origin. In Fig. 8, we observe a similar trend across the Chung plot, indicating that the sampled fluids have a common origin. Using Kharaka and Specht's (1988) method, the Henry constants of the noble gases dissolving into oil have been calculated by modelling the first charge as an oil-like fluid with an API 25^o and methane as a proxy for the lighter drier second charge. These calculations use the average reservoir conditions of 113 °C, 420 bar and salinity of 0.35 M, based on measurements from the three wells drilled and assuming that all hydrocarbons are initially devoid of atmosphere-derived noble gases.

Using these parameters and known charging history, we outline the fractionation of noble gases that will result from a two-stage partitioning model, where an oil partially strips an aquifer of noble gas, followed by a gas stripping an oil. The first hydrocarbon charge of the field can be represented by noble gases partitioning from the aquifer into the oil phase defined by Bosch and Mazor (1988), where

$$\left(\frac{[i]}{Ar}\right)_{oil} = \left(\frac{[i]}{Ar}\right)_{aquifer} \frac{\left(\frac{V_{oil}}{V_{H2O}} + \frac{K^d_{Ar(oil)}}{K^d_{Ar(H2O)}}\right)}{\left(\frac{V_{oil}}{V_{H2O}} + \frac{K^d_{i(oil)}}{K^d_{i(H2O)}}\right)}$$

$([i]/[Ar])_{oil}$ is the ratio of a given noble gas [i] in the oil phase, which is related to the original ratio in the aquifer $([i]/[Ar])_{aquifer}$, the oil/water volume ratio V_{oil}/V_{H2O} and K_i^d is the Henry constant of a given noble gas species. The evolution of $^{20}Ne/^{36}Ar$ and $^{84}Kr/^{36}Ar$ from ASSW in both the oil and gas phase under this scenario is depicted in Fig. 7a.

The second phase of the model is a partial partitioning of the aquifer-derived noble gases from the oil phase which had previously interacted with ASSW ($([i]/Ar)_{oil}$) into a gas phase, representing the second charge of a less dense hydrocarbon fluid. This process is defined using the approach of Bosch and Mazor (1988), where

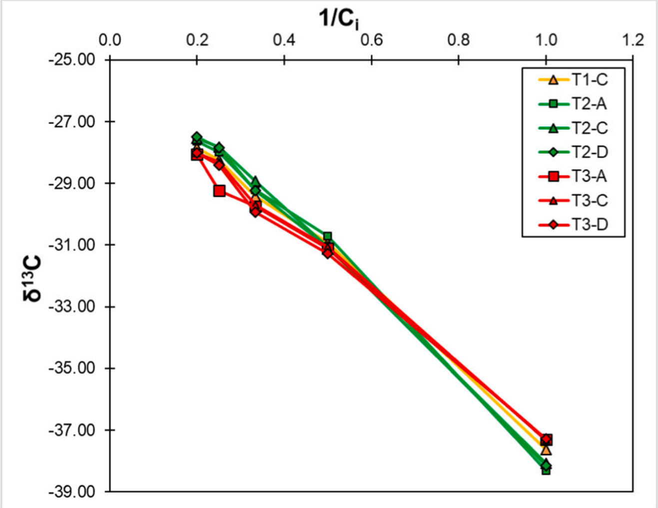

Fig. 8. Chung plot of Tormore samples, where the reciprocal of the carbon number is plotted against $\delta^{13}C$. Samples from all three wells show coevolution with carbon number, indicating all fluids are from the same source.

$$\left(\frac{[i]}{Ar}\right)_{gas} = \left(\frac{[i]}{Ar}\right)_{oil} \frac{\left(\frac{V_{gas}}{V_{H2O}} + \frac{1}{K^d_{Ar}}\right)}{\left(\frac{V_{gas}}{V_{H2O}} + \frac{1}{K^d_{i}}\right)}$$

$([i]/Ar)_{oil}$ is constrained using the data observed from the Tormore field samples as shown in Fig. 7b. The observed $^{20}Ne/^{36}Ar$ and $^{84}Kr/^{36}Ar$ from well T3 define the upper limit of $([i]/Ar)_{oil}$ as a V_{oil}/V_{H2O} of 0.003 and T2 samples define the lower limit of 0.06. Fig. 7b clearly shows that this model exhibits a good fit with the Tormore dataset and hence, we cite that it accurately reflects the charging history of the field. This identification of a likely control on the variation of noble gas composition in the samples, allows resolution that there is a common source of the noble gases throughout the field and explains how noble gas concentrations can vary across the field, but still provide evidence of a fluid connection. In addition, this demonstrates that the distribution of the noble gas is controlled by batch fractionation and therefore we can confidently rule out sample contamination as a cause.

5.2. *Using noble gases to resolve the connectivity of Tormore*

The noble gas composition of a fluid is a record of both the origin and the physical parameters that have acted on it. There are four processes that control the distribution of the noble gases within the field (Fig. 1). In order to establish connection or disconnection within the field, we examine possible causes of differences in the noble gas compositions. Using the geological history of the field, we can constrain the likely processes that are affecting the noble gas composition.

It is assumed that hydrocarbon fluids are fully miscible upon first contact and hence noble gas compositions of the fluids will equilibrate rapidly on contact. Hence, it is valid to rule out a difference in noble gas composition due to the different charging events in different parts of the field. In addition, we account for these differences by fractionation of the noble gases from the double charging of the field. The reservoir is composed of well-sorted turbiditic quartz sands, with a low (< 5%) clay content. The low clay content implies low concentrations of U and Th, meaning that in-situ production of radiogenic noble gases (i.e. ^4He) in the reservoir will be very low compared that of a U and Th rich shale-dominated source rock. C_1/C_2 ratios in Tormore are constant in all reservoir units in the gas phase (Table 3), showing no evidence of fractionation from ongoing charging or leakage (Montel et al., 1993). Hence, the main control of the noble gas fingerprints is the equilibrium conditions of the field, in this case at the OWC. Whilst no OWC was directly encountered during the exploration and appraisal phase of the Tormore field, its presence is observed in the noble gas dataset, due to the increasing concentrations with depth of air saturated water-derived noble gases (^{20}Ne, ^{36}Ar, ^{84}Kr and ^{132}Xe).

5.2.1. *Resolving the vertical connectivity of well T2*

Organic geochemical analysis from field operator reports indicates that reservoir unit T2-A is isolated from the other sands T2-C and T2-D. This is the only currently known direct fluid connection in the Tormore field, and hence is an ideal proof of concept study for assessing the effectiveness of using noble gases to assess reservoir connectivity.

In a virgin reservoir, the atmospheric-derived noble gas composition within the field can only be controlled by fluid column organisation (Fig. 9). In a fully connected reservoir, the noble gases will partition from the aquifer into the hydrocarbons and organise within the accumulation according to the PVT conditions of the field. In the Tormore field, any deviation from this trend is indicative of an absence of connection. In this case, the samples closest to the OWC will have the highest atmosphere-derived component.

In Fig. 9, samples from T2 show a clear linear trend between $^{132}Xe/^{36}Ar$ and $1/^{36}Ar$ which can be explained by each reservoir unit representing a mix of an atmosphere-derived component, likely a

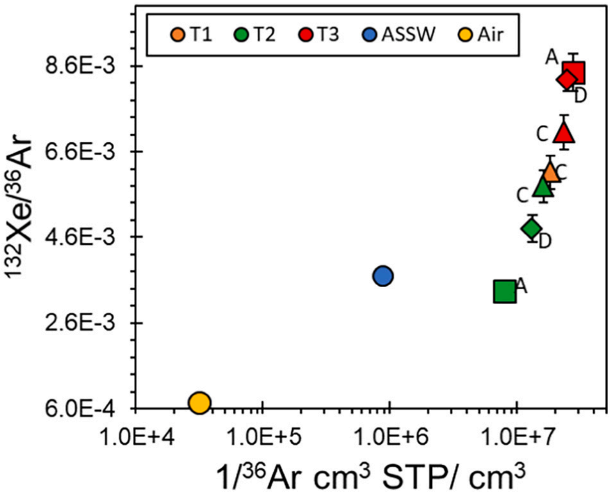

Fig. 9. Plot of $1/^{36}Ar$ against $^{132}Xe/^{36}Ar$ from the Tormore field. Across the field, wells follow the predicted distribution of noble gases, the further from the predicted OWC and ASSW value, the further away each well plot. Uncertainties are 1 σ.

modified atmosphere-derived e.g. ASSW, and an unknown hydrocarbon endmember. This confirms that an underlying aquifer is interacting with all reservoir units in the well. If all reservoir units in well T2 are connected to a common aquifer, this hierarchy would be preserved with depth, where the deepest reservoir unit closest to the OWC will have the highest atmospheric component (Fig. 10). However, this predicted hierarchy is not observed. Instead, T2-A has the closest measured value to the predicted ASSW ratio. This deviation from the predicted trend indicates that T2-A is isolated from the T2-C and T2-D horizons and therefore disconnected suggesting that T2-A is connected with a separate aquifer leg.

Hence, the noble gases and conventional geochemical methods for the oil in T2 both illustrate a disconnection, showing that noble gases can be used to determine disconnected reservoir units. However, we cannot confidently draw any conclusions about the connectivity of T2-C and T2-D. We find no definitive evidence to suggest these units are isolated, and no evidence to suggest they are connected. Hence, the noble gas fingerprint method exhibits the same limitation as established static connectivity tools in this scenario (Table 1).

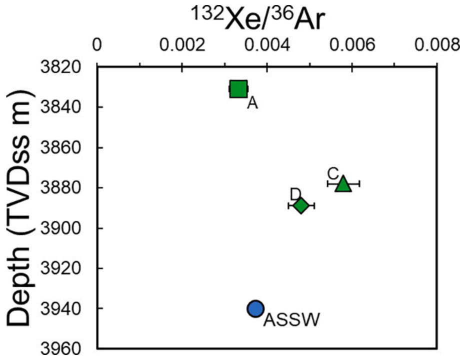

Fig. 10. A plot of $^{132}Xe/^{36}Ar$ against depth. Plotted at the estimated OWC depth is ASSW. When plotted with depth, T2 samples do not follow the predicted trend. T2-A is much closer to the ASSW signature, though it is the shallowest reservoir unit in T2. As a result of this deviation from the predicted trend, we interpret that T2-A is isolated and disconnected vertically from T2-C and T2-D. This result confirms the conclusions drawn from the conventional study on the vertical connectivity of T2 and provides strong evidence of a second OWC in Tormore for reservoir unit T2. Uncertainties are 1 σ. ASSW at 4 °C is after Kipfer et al. (2002).

5.2.2. *Lateral connectivity across a fault*

Seismic studies from the field have identified a normal fault with an unknown offset and transmissibility between wells T2 and T1. As the reservoir units on one side of the fault contain oil and the other gas condensate. The degree of fluid communication across the fault is currently unknown. Hence, there is no knowledge of whether it is acting as a barrier to flow (and therefore the likely location of the GOC), or if it is transmissible, where fluids can communicate across the fault zone on geological timescales (statically connected). Conventional connectivity analysis across the fault has proved inconclusive due to the inability to assess the connectivity between the separate oil and gas phases.

In order to ascertain whether the noble gases can be used to constraint the connectivity, we now examine all the atmosphere-derived noble gases. If the fault is acting as a barrier to flow, then samples up-dip of the fault will be isolated from the underlying aquifer. Due to its isolation, the up-dip compartment (T1-C) will have lower measured atmospheric noble gases, compared to T2 samples. In a scenario where the fault zone is transmissible, there will be a comparable noble gas fingerprint in the fluids from both wells. Fig. 11 shows the atmospheric-derived noble gas isotopes relative to ^{36}Ar and normalised to ASSW from both T2 and the sole reliably sampled reservoir unit of well T1. Firstly, we observe that T2-A (green line with square markers) is isolated from the other T2 samples, supporting our interpretation of a disconnection between the reservoir unit T2-A and the other units in T2.

The noble gas composition of the samples from either side of the fault, T1-C (orange line) and T2-C (green line, triangle markers) are similar. When normalised to ASSW we observe a 5–7% range in T1-C and T2-C, $^{20}Ne/^{36}Ar$, $^{84}Kr/^{36}Ar$ and $^{132}Xe/^{36}Ar$ ratio. This is despite the samples being obtained from two different wells that were drilled 5 years apart, which are located 1.5 km away from each other, separated by a fault and sampled from two different phases. These similarities can only be explained if the reservoir units are in direct and ongoing communication with each other, providing clear evidence that the two reservoir units are connected.

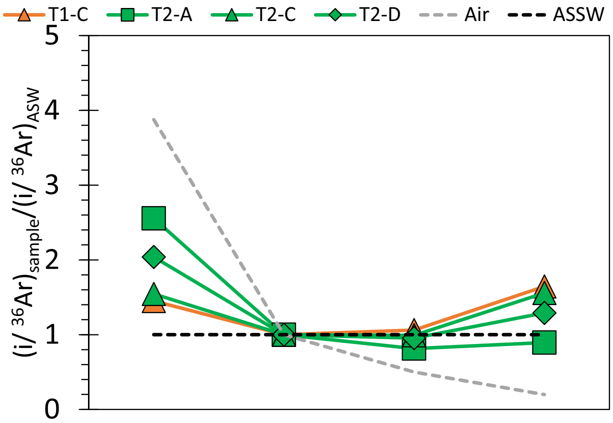

Fig. 11. Spider diagram of atmospheric-derived noble gas isotopes relative to ^{36}Ar and normalised to ASSW. Between wells, T1 and T2 is an antithetic normal fault with an unknown offset and transmissibility. All samples in $^{20}Ne/^{36}Ar$ space plot between ASSW and air. We propose that the high $^{20}Ne/^{36}Ar$ is due to the preferential partitioning of ^{20}Ne in the oil system at the OWC. This plot confirms the isolation of T2-A from the other wells in T2 as it significantly deviates from the trend observed in the other samples. Also, it is evident that T1-C and T2-C have very similar noble gas fingerprints. These samples were taken from the same reservoir unit (separated by a fault), taken from different wells (drilled 5 years apart) show the same fingerprints. From this we can confidently conclude that 1) T1-C and T2-C are in static connectivity and 2) that the fault is transmissible between these two units, and therefore proves a lateral connection.

5.2.3. Lateral connectivity across the Tormore field

No conventional method has confidently resolved the lateral connectivity between the gas-condensate and oil in the Tormore field. After demonstrating the proof of concept of our new noble gas method in the oil column of well T2 and the lateral connectivity of T1 and T2 we now focus on resolving the connectivity across all three wells. Following the same approach used in well T2 we hypothesize that in a fully connected system, in contact with a common aquifer, the distribution of atmosphere-derived noble gases will correlate with depth. We hypothesize that the samples closest to the OWC and aquifer should have higher concentrations of atmosphere-derived noble gases.

In Fig. 9 ^{132}Xe/^{36}Ar is plotted against 1/^{36}Ar illustrating that across all samples we observe a linear trend between a modified atmosphere-derived source e.g. an ASSW that has been modified by the drilling mud, and an unknown hydrocarbon endmember. Based on this trend we would predict that the samples closest to the ASSW endmember should exhibit a depth trend linked to the position of the OWC. However, we find that reservoir unit T3-A does not follow the same trend as the other samples. Hence, we can conclude that T3-A is vertically isolated from the other two reservoir units in T3 and must be in contact with a separate aquifer. However, we are unable to draw any further conclusions for regarding the lateral connectivity of T3-A with the other wells using this method.

Two possible scenarios for the lateral connectivity between well T1 and T3 remain; 1) T3-A is in static connection with well T1 or 2) T3-C and T3-D are in connection with T1. From the methods outlined it is difficult to make any further conclusions. However, there is no evidence of faulting between T1 and T3 that could provide a pathway for noble gases. Therefore, the most likely connection between the wells T1 and T3 based on the known geology is reservoir unit C and D.

In Fig. 12, we model the proportion of additional ASSW noble gases required for the samples from T3 to match that observed in T1. For T3-A an additional 0.03% ASSW-derived noble gas contribution is required and 0.02% for T3-C. Though T3-C requires a smaller addition of atmospheric-derived noble gases than T3-A, to have a similar fingerprint to that observed in T1-C, this is suggestive that T1-C and T3-C are connectivity. However, this is not conclusive evidence for confirming connectivity between the two reservoir units, though the noble gases do provide more information than other static connectivity tools. Hence, this provides useful information on the additional information provided by noble gases in assessing vertical and lateral connectivity between two different phases. The method demonstrates a novel process for assessing static connectivity and readily identifies isolated reservoir units. However, in cases where there is limited data it can be difficult to confirm a definitive connection, especially without dynamic or production data.

6. Conclusions

We conclude that noble gases are potentially an effective tool for resolving the connectivity of hydrocarbon reservoirs. In the Tormore field, we find strong evidence that T2-A is isolated from the other reservoir units of T2, supporting the conclusions of Total's conventional connectivity study. In addition, we find that T3-A is vertically isolated from T3-C and T3-D. These findings demonstrate the applicability of noble gases for assessing the vertical connectivity of reservoir units in both phases.

In addition to resolving the vertical connectivity, we provide strong evidence for resolving the lateral connectivity within the Tormore field. In T1-C and T2-C we find that two noble gas fingerprints from either side of a fault exhibit extremely similar ratios. This is despite samples being obtained from two different wells that were drilled 5 years apart, located 1.5 km away from each other and sampled from two different hydrocarbon phases. The similarities in noble gas fingerprints can only be explained when reservoir units are in direct and ongoing communication, demonstrating noble gases can be used to resolve the static lateral connectivity of fluids in different phases.

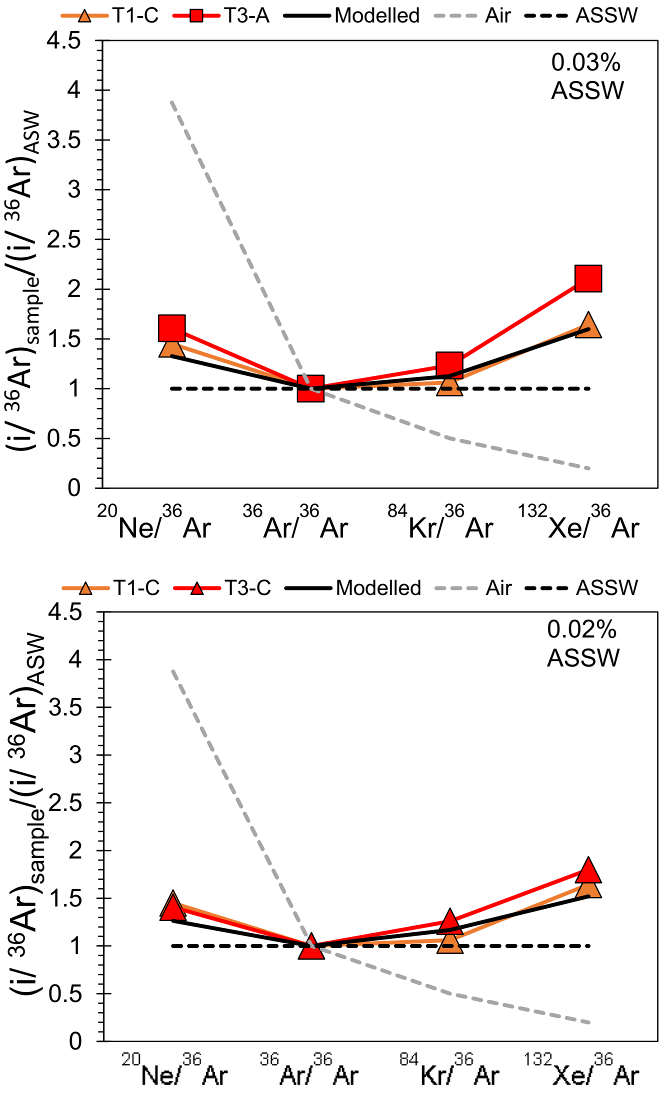

Fig. 12. Spider diagram of atmospheric-derived noble gas isotopes plotted relative to ^{36}Ar and normalised to ASSW. Plotted are reservoir units T1-C (orange) T3-A (red line with square markers), T3-C (red line with triangular markers) and air (grey line). The solid black line represents the amount of ASSW derived noble gases needed for the measured samples of T3 to have similar noble gas fingerprint to T1-C, with the percentage required shown in the corner of the plot. (For interpretation of the references to colour in this figure legend, the reader is referred to the web version of this article.)

It is important to communicate the limitations of this method, which are the same as other conventional tools. It is easy to identify samples that are disconnected, but the converse is not true. Unless samples show extremely similar noble gas fingerprints, it is particularly difficult to prove connectivity between two reservoir units, as demonstrated for establishing the lateral connectivity between T1 and T3. Using noble gases on their own are a powerful tool, but by using additional information to add context to our findings allows us to make better informed interpretations. In this case, the lack of evidence of a conduit connecting T3-A with T1-C suggests that the two reservoir units are unlikely to be connected, hence, it is more likely that T1-C is connected to T3-C, which are within the same reservoir unit with no observed barrier between them.

By sampling fluids directly from each reservoir unit, it is possible to ascertain further information than fluid connectivity. Using the work of Bosch and Mazor (1988) we provide a constraint on the original V_{H20}/V_{oil} ratio. We find a V_{H20}/V_{oil} ratio of 0.003–0.06. This suggests that the first charge of the denser fluid, had not fully stripped the underlying aquifer of noble gases or was still charging when the second drier, less dense fluid charged the Tormore field. Though there is some degree of uncertainty in these values based on the upper and lower limit, this information is invaluable during the exploration phase of a basin and providing a rough estimate of the water/oil ratio is key parameter for basin modelling.

In summary, we have outlined a new source for collecting noble gases from hydrocarbon reservoirs, subsampling from fluids that have been collected downhole from each reservoir unit. In addition, we have demonstrated the application of noble gases for assessing the static vertical and lateral connectivity of hydrocarbon fluids in both the oil and gas phase.

Declaration of Competing Interest

The authors declare that they have no known competing financial interests or personal relationships that could have appeared to influence the work reported in this paper.

Acknowledgments

We are grateful to Total S.A and Total Exploration and Production U.K. for funding, providing samples and permission to publish these results. We would also like to thank Séverine Hourcq for her help collecting samples and Dr. Marta Zurakowska for helping with sample preparation and analysis. Finally, we would like to thank the reviewers Pete Barry, Mike Lawson, Tom Darrah and the two anonymous reviewers for their in-depth feedback who helped improve this manuscript greatly.

References

Aeschbach-Hertig, W., El-Gamal, H., Wieser, M., Palcsu, L., 2008. Modeling excess air and degassing in groundwater by equilibrium partitioning with a gas phase. Water Resour. Res. 44 (8).

Austin, J.A., Cannon, S.J.C., Ellis, D., 2014. Hydrocarbon exploration and exploitation West of Shetlands. Geol. Soc. Lond., Spec. Publ. 397, 1–10.

Ballentine, C.J., Burnard, P.G., 2002. Production, release and transport of noble gases in the continental crust. Rev. Mineral. Geochem. 47 (1), 481–538.

Ballentine, C.J., Hall, C.M., 1999. Determining paleotemperature and other variables by using an error-weighted, nonlinear inversion of noble gas concentrations in water. Geochim. Cosmochim. Acta 63 (16), 2315–2336.

Ballentine, C.J., O'Nions, R.K., Oxburgh, E.R., Horvath, F., Deak, J., 1991. Rare gas constraints on hydrocarbon accumulation, crustal degassing and groundwater flow in the Pannonian Basin. Earth Planet. Sci. Lett. 105 (1–3), 229–246.

Ballentine, C.J., O'Nions, R.K., Coleman, M.L., 1996. A Magnus opus: Helium, neon, and argon isotopes in a North Sea oilfield. Geochim. Cosmochim. Acta 60 (5), 831–849.

Ballentine, C.J., Burgess, R., Marty, B., 2002. Tracing fluid origin, transport and interaction in the crust. Rev. Mineral. Geochem. 47 (1), 539–614.

Barry, P.H., Lawson, M., Meurer, W.P., Warr, O., Mabry, J.C., Byrne, D.J., Ballentine, C.J., 2016. Noble gases solubility models of hydrocarbon charge mechanism in the Sleipner Vest gas field. Geochim. Cosmochim. Acta 194, 291–309.

Barry, P.H., Lawson, M., Meurer, W.P., Danabalan, D., Byrne, D.J., Mabry, J.C., Ballentine, C.J., 2017. Determining fluid migration and isolation times in multiphase crustal domains using noble gases. Geology 45 (9), 775–778.

Barry, P.H., Lawson, M., Meurer, W.P., Cheng, A., Ballentine, C.J., 2018a. Noble gases in deepwater oils of the US Gulf of Mexico. Geochem. Geophys. Geosyst. 19 (11), 4218–4235.

Barry, P.H., Kulongoski, J.T., Landon, M.K., Tyne, R.L., Gillespie, J., Stephens, M., et al., 2018b. Tracing enhanced oil recovery signatures in casing gases using noble gases. Earth Planet. Sci. Lett. 496, 57–67.

Battani, A., Sarda, P., Prinzhofer, A., 2000. Basin scale natural gas source, migration and trapping traced by noble gases and major elements: the Pakistan Indus basin. Earth Planet. Sci. Lett. 181 (1–2), 229–249.

Bosch, A., Mazor, E., 1988. Natural gas association with water and oil as depicted by atmospheric noble gases: case studies from the southeastern Mediterranean Coastal Plain. Earth Planet. Sci. Lett. 87 (3), 338–346.

Brodie, J., White, N., 1994. Sedimentary basin inversion caused by igneous underplating: Northwest European continental shelf. Geology 22 (2), 147–150.

Burnard, P. (Ed.), 2013. The Noble Gases as Geochemical Tracers. Springer, New York, p. 391.

Burnard, P., Graham, D., Turner, G., 1997. Vesicle-specific noble gas analyses of "popping rock": implications for primordial noble gases in Earth. Science 276 (5312), 568–571.

Byrne, D.J., Barry, P.H., Lawson, M., Ballentine, C.J., 2018. Noble gases in conventional and unconventional petroleum systems. Geol. Soc. Lond., Spec. Publ. 468 (1), 127–149.

Byrne, D.J., Barry, P.H., Lawson, M., Ballentine, C.J., 2020. The use of noble gas isotopes to constrain subsurface fluid flow and hydrocarbon migration in the East Texas Basin. Geochim. Cosmochim. Acta 268, 186–208.

Castro, M.C., Goblet, P., Ledoux, E., Violette, S., de Marsily, G., 1998. Noble gases as natural tracers of water circulation in the Paris Basin: 2. Calibration of a groundwater flow model using noble gas isotope data. Water Resour. Res. 34 (10), 2467–2483.

Crovetto, R., Fernández-Prini, R., Japas, M.L., 1982. Solubilities of inert gases and methane in H2O and in D2O in the temperature range of 300 to 600 K. J. Chem. Phys. 76 (2), 1077–1086.

Darrah, T.H., Vengosh, A., Jackson, R.B., Warner, N.R., Poreda, R.J., 2014. Noble gases identify the mechanisms of fugitive gas contamination in drinking-water wells overlying the Marcellus and Barnett Shales. Proc. Natl. Acad. Sci. 111 (39), 14076–14081.

Darrah, T.H., Jackson, R.B., Vengosh, A., Warner, N.R., Whyte, C.J., Walsh, T.B., Poreda, R.J., 2015. The evolution of Devonian hydrocarbon gases in shallow aquifers of the northern Appalachian Basin: insights from integrating noble gas and hydrocarbon geochemistry. Geochim. Cosmochim. Acta 170, 321–355.

Day, J.M., Barry, P.H., Hilton, D.R., Burgess, R., Pearson, D.G., Taylor, L.A., 2015. The helium flux from the continents and ubiquity of low- $^3He/^4He$ recycled crust and lithosphere. Geochim. Cosmochim. Acta 153, 116–133.

Doré, A.G., Lundin, E.R., Birkeland, O., Eliassen, P.E., Jensen, L.N., 1997. The NE Atlantic margin; implications of late Mesozoic and Cenozoic events for hydrocarbon prospectivity. Pet. Geosci. 3 (2), 117–131.

Eberhardt, P., Eugster, O., Marti, K., 1965. A redetermination of the isotopic composition of atmospheric neon. Zeitschrift für Naturforschung A 20 (4), 623–624.

Elshahawi, H., Hasem, M., Mullins, O.C., Fujisawa, G., 2005. The Missing Link – Identification of Reservoir Compartmentalization Through Downhole Fluid Analysis. Society of Petroleum Engineers (SPE Paper 94709).

Elshahawi, H., Venkataramanan, L., McKinney, D., Flannery, M., Mullins, O.C., Hashem, M., 2008. Combining continuous fluid typing, wireline formation testers, and geochemical measurements for an improved understanding of reservoir architecture. SPE Reserv. Eval. Eng. 11 (01), 27–40.

Fanale, F.P., Cannon, W.A., 1971. Physical adsorption of rare gas on terrigenous sediments. Earth Planet. Sci. Lett. 11, 362–368.

Fernández-Prini, R., Alvarez, J.L., Harvey, A.H., 2003. Henry's constants and vapor-liquid distribution constants for gaseous solutes in H 2 O and D 2 O at high temperatures. J. Phys. Chem. Ref. Data 32 (2), 903–916.

Gautheron, C., Moreira, M., 2002. Helium signature of the subcontinental lithospheric mantle. Earth Planet. Sci. Lett. 199 (1–2), 39–47.

Gilfillan, S.M.V., Ballentine, C.J., Holland, G., Blagburn, D., Sherwood Lollar, B., Stevens, S., Schoell, M., Cassidy, M., 2008. The noble gas geochemistry of natural CO_2 gas reservoirs from the Colorado Plateau and Rocky Mountain provinces, USA. Geochim. Cosmochim. Acta 72 (4), 1174–1198.

Gilfillan, S.M.V., Sherwood Lollar, B., Holland, G., Blagburn, D., Stevens, S., Schoell, M., Ballentine, C.J., 2009. Solubility trapping in formation water as dominant CO_2 sink in natural gas fields. Nature 458 (7238), 614.

Gilfillan, S.M.V., Haszedline, S., Stuart, F., Gyore, D., Kilgallon, R., Wilkinson, M., 2014. The application of noble gases and carbon stable isotopes in tracing the fate, migration and storage of CO2. Energy Procedia 63, 4123–4133.

Graham, D.W., 2002. Noble gas isotope geochemistry of mid-ocean ridge and ocean island basalts: Characterization of mantle source reservoirs. Rev. Mineral. Geochem. 47 (1), 247–317.

Györe, D., Stuart, F.M., Gilfillan, S.M.V., Waldron, S., 2015. Tracing injected CO_2 in the Cranfield enhanced oil recovery field (MS, USA) using He, Ne and Ar isotopes. Int. J. Greenhouse Gas Control 42, 554–561.

Györe, D., Gilfillan, S.M.V., Stuart, F.M., 2017. Tracking the interaction between injected CO_2 and reservoir fluids using noble gas isotopes in an analogue of large-scale carbon capture and storage. Appl. Geochem. 78, 116–128.

Harvey, A.H., 1996. Semiempirical correlation for Henry's constants over large temperature ranges. AICHE J. 42 (5), 1491–1494.

Hiyagon, H., Kennedy, B.M., 1992. Noble gases in CH_4-rich gas fields, Alberta, Canada. Geochim. Cosmochim. Acta 56 (4), 1569–1589.

Holland, G., Gilfillan, S., 2013. Application of noble gases to the viability of CO_2 storage. In: The Noble Gases as Geochemical Tracers. Springer, Berlin, Heidelberg, pp. 177–223.

Honda, M., McDougall, I., Patterson, D.B., Doulgeris, A., Clague, D.A., 1991. Possible solar noble-gas component in Hawaiian basalts. Nature 349 (6305), 149.

Honda, M., Zhang, X., Phillips, D., Hamilton, D., Deerberg, M., Schwieters, J.B., 2015. Redetermination of the 21Ne relative abundance of the atmosphere, using a high resolution, multi-collector noble gas mass spectrometer (HELIX-MC Plus). Int. J. Mass Spectrom. 387, 1–7.

Hunt, A.G., Darrah, T.H., Poreda, R.J., 2012. Determining the source and genetic fingerprint of natural gases using noble gas geochemistry: a northern Appalachian Basin case study. AAPG Bull. 96 (10), 1785–1811.

Iliffe, J.E., Robertson, A.G., Ward, G.H.F., Wynn, C., Pead, S.D.M., Cameron, N., 1999. The importance of fluid pressures and migration to the hydrocarbon prospectivity of the Faeroe–Shetland White Zone. In: Geological Society, London, Petroleum Geology Conference Series, Vol. 5(1). Geological Society of London, pp. 601–611.

Jolley, S.J., Fisher, Q.J., Ainsworth, R.B., 2010. Reservoir compartmentalization: an introduction. Geol. Soc. Lond., Spec. Publ. 347 (1), 1–8.

Kaufman, R.L., Kabir, C.S., Abdul-Rahman, B., Quttainah, R., Dashtl, H., Pederson, J.M., Moon, M.S., 1990. Characterizing the Greater Burgan field with geochemical and other field data. Soc. Petrol. Eng. Reserv. Eng. Eval. 3, 118–126.

Kennedy, B.M., Hiyagon, H., Reynolds, J.H., 1990. Crustal neon: a striking uniformity. Earth Planet. Sci. Lett. 98 (3–4), 277–286.

Kharaka, Y.K., Specht, D.J., 1988. The solubility of noble gases in crude oil at 25–100 °C. Appl. Geochem. 3 (2), 137–144.

Kipfer, R., Aeschbach-Hertig, W., Peeters, F., Stute, M., 2002. Noble gases in lakes and ground waters. Rev. Mineral. Geochem. 47 (1), 615–700.

König, H., Wänke, H., Bien, G.S., Rakestraw, N.W., Suess, H.E., 1964. Helium, neon and argon in the oceans. In: Deep Sea Research and Oceanographic Abstracts, Vol. 11(2), pp. 243–247.

Lee, J.Y., Marti, K., Severinghaus, J.P., Kawamura, K., Yoo, H.S., Lee, J.B., Kim, J.S., 2006. A redetermination of the isotopic abundances of atmospheric Ar. Geochim. Cosmochim. Acta 70 (17), 4507–4512.

Mamyrin, B.A., Anufrijev, G.S., Kamenskii, I.l., Tolstikhin, I.N., 1970. Determination of the isotopic composition of atmospheric helium. Geochem. Int. 7, 498–505.

Mark, D.F., Stuart, F.M., De Podesta, M., 2011. New high-precision measurements of the isotopic composition of atmospheric argon. Geochim. Cosmochim. Acta 75 (23), 7494–7501.

Montel, F., Caillet, G., Puchea, A., Caltagirone, J.P., 1993. Diffusion model for predicting reservoir gas losses. Mar. Pet. Geol. 10, 51–57.

Moreira, M., Allègre, C.J., 1998. Helium–neon systematics and the structure of the mantle. Chem. Geol. 147 (1–2), 53–59.

Morrison, P., Pine, J., 1955. Radiogenic origin of the helium isotopes in rock. Ann. N. Y. Acad. Sci. 62 (3), 71–92.

Naylor, P.H., Bell, B.R., Jolley, D.W., Durnall, P., Fredsted, R., 1999. Palaeogene magmatism in the Faeroe–Shetland Basin: influences on uplift history and sedimentation. In: Geological Society, London, Petroleum Geology Conference Series, Vol. 5(1). Geological Society of London, pp. 545–558.

O'Nions, R.K., Oxburgh, E.R., 1988. Helium, volatile fluxes and the development of continental crust. Earth Planet. Sci. Lett. 90 (3), 331–347.

Oxburgh, E.R., O'Nions, R.K., Hill, R.I., 1986. Helium isotopes in sedimentary basins. Nature 324 (6098), 632.

Ozima, M., Podosek, F.A., 2002. Noble Gas Geochemistry, 2nd ed. Cambridge University Press.

Peeters, F., Livingstone, D.M., Goudsmit, G.H., Kipfer, R., Forster, R., 2002. Modeling 50 years of historical temperature profiles in a large central European lake. Limnol. Oceanogr. 47 (1), 186–197.

Pinti, D.L., Marty, B., 1995. Noble gases in crude oils from the Paris Basin, France: implications for the origin of fluids and constraints on oil-water-gas interactions. Geochim. Cosmochim. Acta 59 (16), 3389–3404.

Prinzhofer, A., 2013. Noble gases in oil and gas accumulations. In: The Noble Gases as Geochemical Tracers. Springer, Berlin, Heidelberg, pp. 225–247.

Prinzhofer, A., Battani, A., 2003. Gas isotopes tracing: an important tool for hydrocarbons exploration. Oil Gas Sci. Technol. 58 (2), 299–311.

Pujol, M., Van den Boorn, S., Bourdon, B., Brennwald, M., Kipfer, R., 2018. Physical processes occurring in tight gas reservoirs from Western Canadian Sedimentary Basin: noble gas signature. Chem. Geol. 480, 128–138.

Ritchie, J.D., Hitchen, K., 1987. Geological review of the West Shetland area. In: Brooks, J., Glennie, K.W. (Eds.), Petroleum Geology of Northwest Europe, pp. 737–749.

Sarda, P., Staudacher, T., Allègre, C.J., 1988. Neon isotopes in submarine basalts. Earth Planet. Sci. Lett. 91 (1–2), 73–88.

Smalley, P.C., Muggeridge, A.H., 2010. Reservoir Compartmentalization: get it before it gets you. Geol. Soc. Lond., Spec. Publ. 347, 25–41.

Snedden, J.W., Vrolijk, P., Sumpter, L., Sweet, M.L., Barnes, K.R., White, E., Farrell, M.E., 2007. Reservoir connectivity: definitions, strategies, and applications. In: International Petroleum Technology Conference.

Tolstikhin, I.N., Ballentine, C.J., Polyak, B.G., Prasolov, E.M., Kikvadze, O.E., 2017. The noble gas isotope record of hydrocarbon field formation time scales. Chem. Geol. 471, 141–152.

Torgersen, T., Kennedy, B.M., van Soest, M.C., 2004. Diffusive separation of noble gases and noble gas abundance patterns in sedimentary rocks. Earth Planet. Sci. Lett. 226 (3–4), 477–489.

Tyne, R.L., Barry, P.H., Hillegonds, D.J., Hunt, A.G., Kulongoski, J.T., Stephens, M.J., Byrne, D.J., Ballentine, C.J., 2019. A novel method for the extraction, purification, and characterization of noble gases in produced fluids. Geochem. Geophys. Geosyst. 20 (11), 5588–5597.

Wagner, W., Pruss, A., 1993. International equations for the saturation properties of ordinary water substance. Revised according to the international temperature scale of 1990. Addendum to J. Phys. Chem. Ref. Data 16, 893 (1987). J. Phys. Chem. Ref. Data 22 (3), 783–787.

Warr, O., Sherwood Lollar, B., Fellowes, J., Sutcliffe, C.N., McDermott, J.M., Holland, G., Mabry, J.C., Ballentine, C.J., 2018. Tracing ancient hydrogeological fracture network age and compartmentalisation using noble gases. Geochim. Cosmochim. Acta 222, 340–362.

Weiss, R.F., 1970. The solubility of nitrogen, oxygen and argon in water and seawater. In: Deep Sea Research and Oceanographic Abstracts, Vol. 17(4), pp. 721–735.

White, R., McKenzie, D., 1989. Magmatism at rift zones: the generation of volcanic continental margins and flood basalts. J. Geophys. Res. 94 (B6), 7685–7729.

Zaikowski, A., Spangler, R.R., 1990. Noble gas and methane partitioning from ground water: an aid to natural gas exploration and reservoir evaluation. Geology 18 (1), 72–74.

Zhou, Z., Ballentine, C.J., Kipfer, R., Schoell, M., Thibodeaux, S., 2005. Noble gas tracing of groundwater/coalbed methane interaction in the San Juan Basin, USA. Geochim. Cosmochim. Acta 69 (23), 5413–5428.